Copy No. _____

Defence Research and Development Canada
Recherche et développement pour la défense Canada

DEFENCE R&D DÉFENSE

Array Element Localization of a Rapidly Deployable System of Sensors

AEL Final Report for the RDS TDP

Gordon R. Ebbeson
Garry J. Heard
Francine Desharnais
Marie-Noël R. Matthews [a]

Defence Research and Development Canada – Atlantic

[a]*Now at Department of Oceanography*
Dalhousie University, Halifax, NS

Stan E. Dosso
School of Earth and Ocean Sciences
University of Victoria, Victoria, BC

Defence R&D Canada – Atlantic

Technical Memorandum
DRDC Atlantic TM 2007-009
August 2007

Canada

This page intentionally left blank.

Array Element Localization of a Rapidly Deployable System of Sensors

AEL Final Report for the RDS TDP

Gordon R. Ebbeson
Garry J. Heard
Francine Desharnais
Marie-Noël R. Matthews[a]

Defence Research and Development Canada – Atlantic
[a] Now at Department of Oceanography
Dalhousie University, Halifax, NS

Stan E. Dosso

School of Earth and Ocean Sciences
University of Victoria, Victoria, BC

Defence R&D Canada – Atlantic

Technical Memorandum

DRDC Atlantic TM 2007-009

August 2007

Author

Original signed by Gordon R. Ebbeson

Gordon R. Ebbeson

Approved by

Original signed by Neil Sponagle

Neil Sponagle

Head, Underwater Sensing

Approved for release by

Original signed by J. L. Kennedy

Kirk Foster

DRP Chair

Abstract

The Rapidly Deployable Systems (RDS) Technology Demonstration Project (TDP) was a major research effort that was conducted by Defence Research and Development Canada (DRDC) – Atlantic. The purpose of this project was to develop a deployable array system with on-board processing components that would be capable of detecting, localizing, and eventually classifying sources of acoustic and electromagnetic energy traveling on or underneath the sea surface. A difficult requirement for the success of the RDS TDP was that the locations of the deployed array sensors must be known with considerable accuracy, generally with an uncertainty of less than 1 m. This sensor localization requirement arose due to a need to accurately localize the source of signal energy, in particular, the depth of the source. This paper describes and demonstrates a technique referred to as Array Element Localization (AEL) that was developed to solve the sensor localization problem.

Résumé

Initiative de recherche d'envergure de Recherche et développement pour la défense Canada (RDDC) – Atlantique, le projet de démonstration de technologies (TDP) des systèmes à déploiement rapide (RDS) avait pour but de développer un réseau déployable équipé de composantes de traitement embarquées aptes à détecter, localiser et classer ultérieurement des sources de l'énergie acoustique et électromagnétique se déplaçant sur ou sous la surface de la mer. L'une des difficultés majeures du projet RDS TDP tenait à ce que l'emplacement des capteurs déployés devait être connu avec beaucoup d'exactitude, en général à moins d'un mètre près. Ce besoin de précision était surgi lorsqu'il s'est agi de localiser exactement la source de l'énergie de signaux et, en particulier, la profondeur de la source. Le présent document présente une technique de localisation d'éléments de réseau (AEL) pour résoudre le problème de localisation de capteurs.

This page intentionally left blank.

Executive summary

Introduction

The Rapidly Deployable Systems (RDS) Technology Demonstration Project (TDP) was a major research effort that was conducted by Defence Research and Development Canada (DRDC) – Atlantic. The purpose of this project was to develop a deployable array system with on-board processing components that would be capable of detecting, localizing, and eventually classifying sources of acoustic and electromagnetic energy traveling on or underneath the sea surface. A difficult requirement for the success of the RDS TDP was that the locations of the deployed array sensors must be known with considerable accuracy, generally with an uncertainty of less than 1 m. This sensor localization requirement arose due to a need to accurately localize the source of signal energy, in particular, the depth of the source. This paper describes and demonstrates a technique referred to as Array Element Localization (AEL) that was developed to solve the sensor localization problem.

Results

The AEL process consists of estimating the three-dimensional (3D) positions for the hydrophones of an array. It is based on the linearized inversion of the measured arrival time data from a series of controlled impulse sources activated in a pattern around the array and uses the method of regularization to include *a priori* information such as the approximate positions of the sources and hydrophones.

To demonstrate the overall AEL process, the algorithm was used to localize the sensors of a Horizontal Line Array (HLA) denoted as HLA2 during the RDS demonstration trial. The results indicated that the array was deployed in a slight “S” shape with average offsets of -5.4 m in northing and -11.2 m in easting from the estimated deployment location.

Significance

This paper has shown that AEL is a fast and effective algorithm for localizing the hydrophones of the RDS horizontal arrays.

Future plans

The AEL algorithm is essentially complete and there are no future plans to modify the procedure.

Ebbeson, G.R., Heard, G.J., Desharnais, F., Matthews, M.N.R., Dosso, S.E. 2007. Array Element Localization of a Rapidly Deployable System of Sensors. DRDC Atlantic TM 2007-009. Defence R&D Canada - Atlantic.

Sommaire

Introduction

Initiative de recherche d'envergure de Recherche et développement pour la défense Canada (RDDC) – Atlantique, le projet de démonstration de technologies (TDP) des systèmes à déploiement rapide (RDS) avait pour but de développer un réseau déployable équipé de composantes de traitement embarquées aptes à détecter, localiser et classer ultérieurement des sources de l'énergie acoustique et électromagnétique se déplaçant sur ou sous la surface de la mer. L'une des difficultés majeures du projet RDS TDP tenait à ce que l'emplacement des capteurs déployés devait être connu avec beaucoup d'exactitude, en général à moins d'un mètre près. Ce besoin de précision était surgi lorsqu'il s'est agi de localiser exactement la source de l'énergie de signaux et, en particulier, la profondeur de la source. Le présent document présente une technique de localisation d'éléments de réseau (AEL) pour résoudre le problème de localisation de capteurs.

Les résultats

Le processus AEL consiste à estimer les positions tridimensionnelles (3D) des hydrophones d'un réseau. Il est basé sur une inversion linéarisée des données sur l'heure d'arrivée mesurée à partir d'une panoplie de sources d'impulsions contrôlées impulsées par un modèle articulé autour du réseau; il utilise le procédé de régularisation pour les données *a priori* telles que les positions approximatives des sources et des hydrophones.

Pour faire la démonstration du processus global d'AEL, on a utilisé pour le RDS un algorithme afin de localiser les capteurs d'un réseau linéaire horizontal (HLA), dénommés HLA2. À la lumière des résultats, il s'est avéré que le réseau se déployait en S (forme légère), les décalages se situant en moyenne à –5,4 m vers le nord à –11,2 m vers le sud de l'emplacement estimé.

La signification

Le présent document a démontré que l'AEL est un algorithme rapide et efficace pour ce qui est de localiser les hydrophones de réseaux horizontaux du RDS.

Le futur

L'algorithme d'AEL étant pour l'essentiel au point, l'on ne prévoit pas de modifier le processus à l'avenir.

Ebbeson, G.R., Heard, G.J., Desharnais, F., Matthews, M.N.R., Dosso, S.E. 2007. *Array Element Localization of a Rapidly Deployable System of Sensors*. DRDC Atlantic TM 2007-009. Defence R&D Canada - Atlantic.

Table of contents

List of figures

List of tables

This page intentionally left blank.

1. Introduction

The Rapidly Deployable Systems (RDS) Technology Demonstration Project (TDP) was a major research effort that was conducted by Defence Research and Development Canada (DRDC) – Atlantic [1]. The purpose of this project was to develop a deployable array system with on-board processing components that would be capable of detecting, localizing, and eventually classifying sources of acoustic and electromagnetic energy traveling on or underneath the sea surface. The TDP started in February 2002 and a contract was awarded to MacDonald Dettwiler and Associates (MDA) in November 2003. The project ended with a demonstration sea trial in May 2006. However, it should be noted that the TDP was preceded by a lengthy period of in-house research that started as early as 1998. A difficult requirement for the success of the RDS TDP was that the locations of the deployed array sensors must be known with considerable accuracy, generally with an uncertainty of less than 1 m. This sensor localization requirement arose due to a need to accurately localize the source of signal energy, in particular, the depth of the source. This paper describes and demonstrates a technique referred to as Array Element Localization (AEL) that was developed to solve the sensor localization problem.

AEL uses the inversion of acoustic time-of-arrival measurements from a set of controlled impulse sources as received on the hydrophones that require localization. The technique is usually based on the difference in the travel times of the direct arrivals, that is, the sound that travels directly from a source to a receiver. However, it can also include the travel time differences of the surface-reflected and bottom-reflected arrivals, assuming that these arrivals can be readily identified. If the source impulse times are also known, then the inversion can provide even more information.

This paper describes the AEL theory and provides an example of localizing a deployed array of hydrophones using the time delays of the direct arrivals. The technique illustrated makes use of imploding light bulbs at depth as a convenient source of broadband acoustic energy. It must be realized that this is not a suggested method for an operationally deployed array system. An operational array would be localized using the same theory, but with a method that is both fast and covert. During the RDS project, experiments were carried out to test a prototype AEL method for an operational array. That method used of an Autonomous Underwater Vehicle (AUV) [2] carrying a compact, low-frequency impulsive sound source to conduct an AEL survey in a somewhat more clandestine manner than the light bulb method.

In this paper, Section 2 gives an overview of the AEL technique. It includes references for those readers who require more detail. Section 3 describes the AEL experiments that were carried out during the RDS demonstration trial. Then, an example of the AEL procedure using the time delays of the direct arrivals is given in Section 4. It focuses on one of the RDS demonstration arrays and describes both the autonomous pre-processing of the AEL source signatures within the array and the array localization processing at the operator station. This is followed by a Monte Carlo appraisal of the localization uncertainties. Finally, Section 5 summarizes the results.

2. Array Element Localization

AEL acoustic surveys that are used to localize an array of hydrophones after the array has been deployed generally involve measuring the arrival times of the signals transmitted from a series of impulsive sources to the hydrophones that are to be localized. Given the knowledge of the sound speed profile in the ocean and the positions of the sources, these arrival times can be inverted to produce estimates of the array hydrophone locations. If the array is deployed on the sea floor, such as would be the case with a Horizontal Line Array (HLA), this inversion only has to be done once. However, if the array is a Vertical Line Array (VLA) that has been deployed in the water column, then the inversions have to be carried out continuously as the array moves with the currents [3]. In this paper, the method is used to localize an HLA.

2.1 Prior Estimates and Uncertainties

An AEL inversion is a nonlinear operation and therefore there are an infinite number of acceptable models that can fit the measured arrival time data. Hence, the model that *minimizes* the misfit to the measured data, subject to stability constraints which serve to keep the model close to some initial model, is usually considered to be the best solution. The AEL inversion technique described here is based on a slightly different approach. Instead of minimizing the misfit to the arrival time data, the inversion is set up to achieve a misfit that is statistically consistent with the estimated uncertainties of this data, while applying additional independent *a priori* information about the solution to the inversion [4]. This technique has the advantage in that it avoids choosing a model which has a misfit that is smaller than that defined by the uncertainty of the measured data. Ideally, the AEL inversion should address all sources of error in the environment and the acoustic survey and use all physical *a priori* information about the solution. As an example, consider the case of a bottom-mounted HLA. The exact positions and depths of both the sources and hydrophones are unknown. However, *a priori* information about these parameters, that is, their nominal deployment locations, are often available after the survey. In addition, if the array deployment was well controlled, it is quite likely that the array was laid with a high degree of smoothness. This adds further information to the AEL process. Finally, any uncertainties in the sound speed profile due to inexact instrument calibrations and variability of the ocean environment can also be included in the inversion. If all of this information is included and the corresponding uncertainties are kept as small as possible, the AEL technique will yield a significantly accurate result.

2.2 Rayfast Eigenray Model

An important part of the AEL inversion process is the ray tracing model that is used to calculate the predicted eigenray paths and associated arrival travel times that are used to compare to the measured arrival time data. The inversion technique that is described here uses the Rayfast model [5,6]. This model is designed to determine the specific eigenrays of interest in an AEL-type problem in a highly efficient manner. These eigenrays are the rays that travel from a specific source to a specific receiver. With Rayfast, they can include direct rays and reflected rays with up to three surface reflections and two bottom reflections. In this model, the initial eigenrays are estimated using straight lines traced through an isovelocity medium. The harmonic mean of the measured sound speed profile is used for the isovelocity value because it is the best constant representation of the profile. Any reflected rays are handled through the method of images. From

this starting point, Newton's method is used to iteratively search for the eigenray that connects the source to the receiver through the true sound speed medium. Since Newton's method converges quadratically near the solution, this is a highly efficient method of determining eigenrays to high precision, often requiring only one or two iterations. Once the eigenray path length has been determined, the modeled travel time along the ray path can be computed.

2.3 AEL Inversion

An AEL inversion produces an estimate of the three-dimensional (3D) positions for the array hydrophones and impulsive sources included in the localization process. The procedure used here is based on the linearized inversion of the measured arrival time data and uses the method of regularization to include *a priori* information [4-7].

Consider an AEL survey in which there are N_h hydrophones, N_s sources and N_p eigenray paths from each source to each receiver. The acoustic arrival times $\mathbf{t}$ that are measured at the array can be written in vector form as

$$\mathbf{t} = \mathbf{T}(\mathbf{m}) + \mathbf{n} . \tag{1}$$

In (1), $\mathbf{m}$ represents the unknown parameters for the inversion, such as, the source and receiver positions, source instant and/or sound speed bias. The vector $\mathbf{T}(\mathbf{m})$ represents the modeled arrival travel times for the acoustic signals traveling along ray paths between the sources and the hydrophones. Finally, $\mathbf{n}$ represents additive noise errors with the assumption that the error n_i on datum t_i is due to an independent, Gaussian-distributed random process with zero mean and standard deviation σ_i. The standard least-squares solution for this problem is determined by minimizing the χ^2 misfit

$$\chi^2 = \left|\mathbf{G}\left(\mathbf{T}(\mathbf{m}) - \mathbf{t}\right)\right|^2 , \tag{2}$$

where $\mathbf{G} = \mathrm{diag}\left[1/\sigma_i\right]$ represents the influence of the noise errors.

The inverse problem of finding $\mathbf{m}$ from (2) given a measurement of $\mathbf{t}$ is functionally a non-linear problem. However, a local *linearization* can be obtained by expanding $\mathbf{T}(\mathbf{m})$ in a Taylor series to the first order about an arbitrary starting model $\mathbf{m}_0$. That is, consider

$$\mathbf{T}(\mathbf{m}) = \mathbf{T}(\mathbf{m}_0) - \mathbf{J}\mathbf{m}_0 + \mathbf{J}\mathbf{m} , \tag{3}$$

where $\mathbf{J}$ is the Jacobian matrix of partial derivatives $J_{ij} = \partial T_i(\mathbf{m}_0)/\partial m_j$. From (1) and (3) it can be shown that

$$\mathbf{t} - \mathbf{T}(\mathbf{m}_0) + \mathbf{J}\mathbf{m}_0 = \mathbf{J}\mathbf{m} + \mathbf{n} \equiv \mathbf{d} , \tag{4}$$

where $\mathbf{d}$ represents the modified measured data in terms of known quantities. This equation represents a linear inverse problem that has a least-squares solution for $\mathbf{m}$ that can be found by minimizing the χ^2 misfit

$$\chi^2 = \left|\mathbf{G}\left(\mathbf{Jm} - \mathbf{d}\right)\right|^2. \tag{5}$$

However, because the nonlinear terms have been neglected, this inversion must be repeated iteratively while monitoring for convergence.

In this AEL inversion, where both the hydrophone and source positions are treated as unknowns, the measured arrival time data alone do not necessarily constrain the solution. More information is required. The method of *regularization* is a powerful tool in which *a priori* information can be included in the linear inversion. For the localization of a horizontal array, there are typically two different forms of prior information. Hence, two regularization terms can be added to the data misfit of (5) to form a new objective function for minimization:

$$\phi^2 = \left|\mathbf{G}\left(\mathbf{Jm} - \mathbf{d}\right)\right|^2 + \mu_1\left|\mathbf{H}_1\left(\mathbf{m} - \hat{\mathbf{m}}_1\right)\right|^2 + \mu_2\left|\mathbf{H}_2\left(\mathbf{m} - \hat{\mathbf{m}}_2\right)\right|^2. \tag{6}$$

In this equation $\hat{\mathbf{m}}_1$ and $\hat{\mathbf{m}}_2$ represent the prior data, $\mathbf{H_1}$ and $\mathbf{H_2}$ are the regularization matrices for the prior estimates of that data, and μ_1 and μ_2 are trade-off parameters which determine the relative importance of the prior information. The first regularization matrix, $\mathbf{H}_1$, applies prior parameter estimates for the source and receiver positions as available from the array deployment procedure. Hence, $\hat{\mathbf{m}}_1$ consists of the prior estimates for those positions and $\mathbf{H}_1$ would weight these estimates according to their uncertainties. That is, $\mathbf{H}_1 = \mathrm{diag}\left[1/u_i\right]$, where u_i is the standard deviation of an assumed Gaussian uncertainty distribution for the *i*th parameter estimate $\hat{m}_{1i}$. The second regularization matrix, $\mathbf{H_2}$, applies the *a priori* expectation that the array shape is a smooth function, that is, there is minimal curvature along the length of the array. In this case, $\hat{\mathbf{m}}_2 = 0$ and $\mathbf{H_2}$ consists of a tridiagonal matrix with nonzero entries on the *i*th row given by

$$\mathbf{H}_2 = \mathrm{diag}\left[\frac{-1}{\left(v_{i+1} - v_i\right)^2}, \frac{v_{i+2} - v_i}{\left(v_{i+2} - v_{i+1}\right)\left(v_{i+1} - v_i\right)^2}, \frac{-1}{\left(v_{i+2} - v_{i+1}\right)\left(v_{i+1} - v_i\right)}\right], \tag{7}$$

where v_i represents the expected 3D offset along the array to the *i*th receiver. Using $\mathbf{H_2}$ provides the simplest array shape that is consistent with the acoustic data and prior position estimates.

Minimizing the objective function of (6) with respect to $\mathbf{m}$ leads to the solution

$$\mathbf{m} = \left[\mathbf{J}^T\mathbf{G}^T\mathbf{GJ} + \mu_1\mathbf{H}_1^T\mathbf{H}_1 + \mu_2\mathbf{H}_2^T\mathbf{H}_2\right]^{-1} \times \left[\mathbf{J}^T\mathbf{G}^T\mathbf{Gd} + \mu_1\mathbf{H}_1^T\mathbf{H}_1\hat{\mathbf{m}}_1 + \mu_2\mathbf{H}_2^T\mathbf{H}_2\hat{\mathbf{m}}_2\right]. \tag{8}$$

The implementation of the AEL algorithm consists of running an iterative application of the regularized inversion shown in (8), initiated from a starting model that is made up of the prior parameter estimates. The algorithm is considered to have converged if two criteria have been met. For the first criteria, the measured arrival time data must fit with the modeled data such that the χ^2 misfit achieves its expected value of $\left\langle \chi^2 \right\rangle = N_h \times N_s \times N_p$. However, it should be noted that although (8) is derived based on the misfit for the linear inverse problem as shown in (5), the convergence of the inversion algorithm must be judged in terms of the nonlinear misfit shown in (2). For the second criteria, the RMS change in the receiver positions between iterations must be small compared to the desired accuracy of the solution.

Once the solution for the inverse problem has been found, it is possible to estimate the uncertainty of that solution. For problems with Gaussian-distributed data errors and prior estimates, the covariance matrix for the model is given by

$$\mathbf{C} = \left[\mathbf{J}^T\mathbf{G}^T\mathbf{G}\mathbf{J} + \mathbf{H}_1^T\mathbf{H}_1\right]^{-1}, \tag{9}$$

where $\mathbf{J}$ and $\mathbf{G}$ are as defined earlier and $\mathbf{H_1}$ is the regularization matrix for the prior source and receiver positions as described above. The *i*th diagonal element of $\mathbf{C}$ represents the square of the standard deviation of the *i*th recovered parameter. The validity of this approach depends on the degree of nonlinearity of the inverse problem. However, generally it has been found to be an efficient way to evaluate the AEL inversion results.

3. Array Localization Trial

Many RDS trials were carried out near Halifax NS between the fall of 2002 and the spring of 2006. During each of those trials, the array hydrophones were localized with the AEL routines. In all but the last trial, the sensor localizations were carried out in a post-processing mode because the AEL data files were not accessible until the array Pressure Vessels (PVs) were recovered at the end of the trials. However, during the final RDS demonstration trial that was carried out in St. Margaret's Bay during the spring of 2006, the AEL data files were pre-processed on board the array processors installed in the PVs so that a reduced data set could be transmitted via a Radio Frequency (RF) link to the "shore station" located on the research ship *CFAV Quest*. In this way, it was possible to complete the AEL process while the arrays were still deployed.

To demonstrate this overall AEL process, the remainder of this paper concentrates on the localization of a horizontal array denoted as HLA2 during the RDS demonstration trial. Figure 1 shows the location of HLA2 and the other arrays during that trial. The water depth at this site was nominally 69 m and the sea bottom consisted of a thick layer of fine clay-silt sediment.

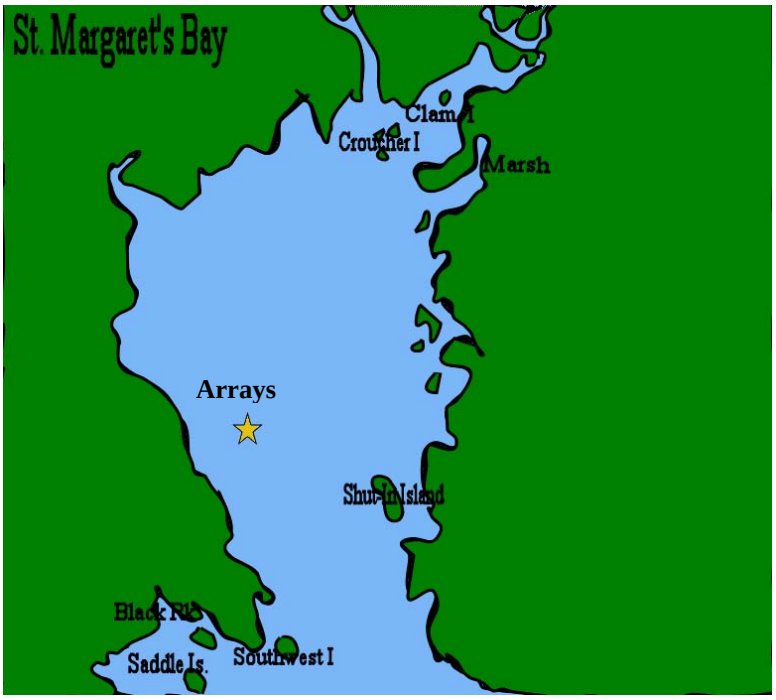

Figure 1. The location of the RDS arrays in St. Margaret's Bay.

Figure 2 shows the configuration of HLA2 from the connector on the PV that contained the recording electronics to the end that was attached to the anchor. The array contained 34 hydrophones for an overall length of 196.65 m from hydrophone H01 to hydrophone H34. Within that length were three, eight-element sub-arrays with nominal hydrophone spacings of 1.2 m, one at either end (H01 to H08 and H27 to H34) and one in the middle (H14 to H20). The array was designed in this manner so that beamforming could be carried out over the entire array, and/or

over each sub-array. This latter option allows for inter-array, bearing cross-fixing of an acoustic source. The goal of the AEL procedure is to determine the inter-element spacings of all of the hydrophones as well as the global position and shape of the array. The array also contained two Underwater Electric Potential (UEP) electrodes and three magnetometers (M01 to M03). These sensors were localized using their positions with respect to the hydrophones. In the analysis that follows, only the positions of the hydrophones will be given.

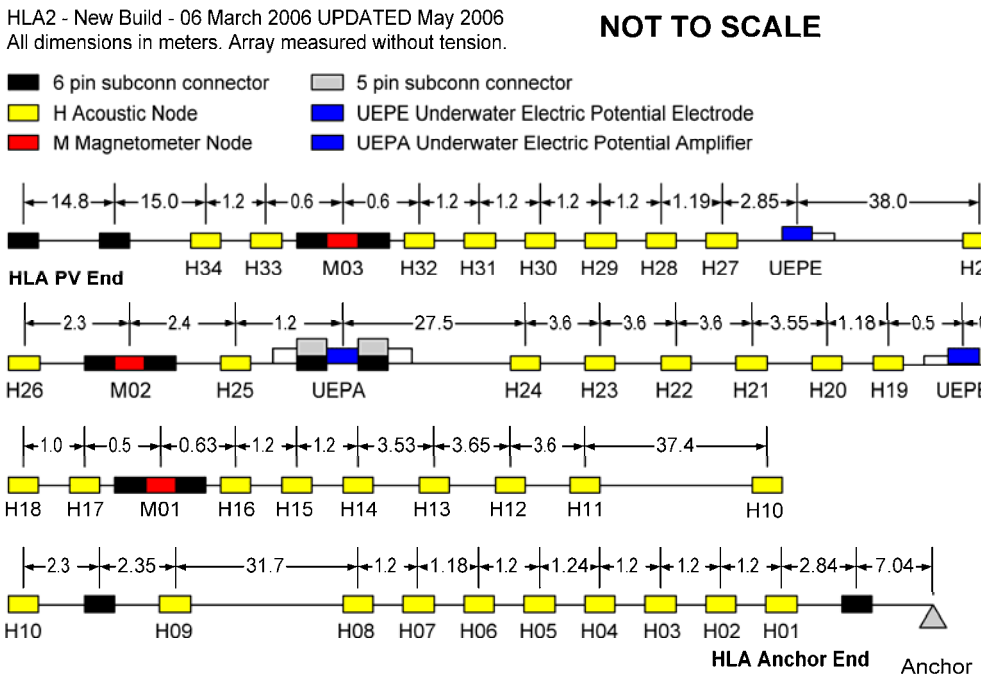

Figure 2. The configuration of horizontal array HLA2.

The deployment of the array is the first critical step in the AEL process. For the best localization accuracy, it is necessary to get good estimates of the array lay-down positions. This is achieved through the use of the deployment sled shown in Fig. 3. During the deployment, the sled is towed about 2 to 3 m above the sea floor. The array anchor is electronically released first. When the anchor reaches the sea floor, the array is slowly pulled off of the deployment tubes located on the back of the sled. When the last portion of the array leaves the tubes, it pulls a pin to release the PV which then falls to the sea floor trailing an acoustic communications modem. The PV, in turn, pulls a communication cable off of the smaller tubes located on the front of the sled. A float brings the end of that cable to the surface so that it can be attached to a monitoring buoy or to a cable running to a shore station. Cameras on the sled allow the deployment progress to be monitored and ensure that accurate timing measurements are made so that the best possible Global Positioning System (GPS) positions of both the anchor and the PV can be recorded.

The next critical step in the AEL process is the deployment of the AEL impulsive sources. For the demonstration trials, the acoustic impulses were generated by imploding light bulbs [8]. The implosion of a light bulb in the water column generates an impulse that can be received on each of the hydrophones in the array. It is the relative time delays of the impulse arriving along the array that are used by the AEL inversion algorithms. Figure 4 shows a light bulb that is about to

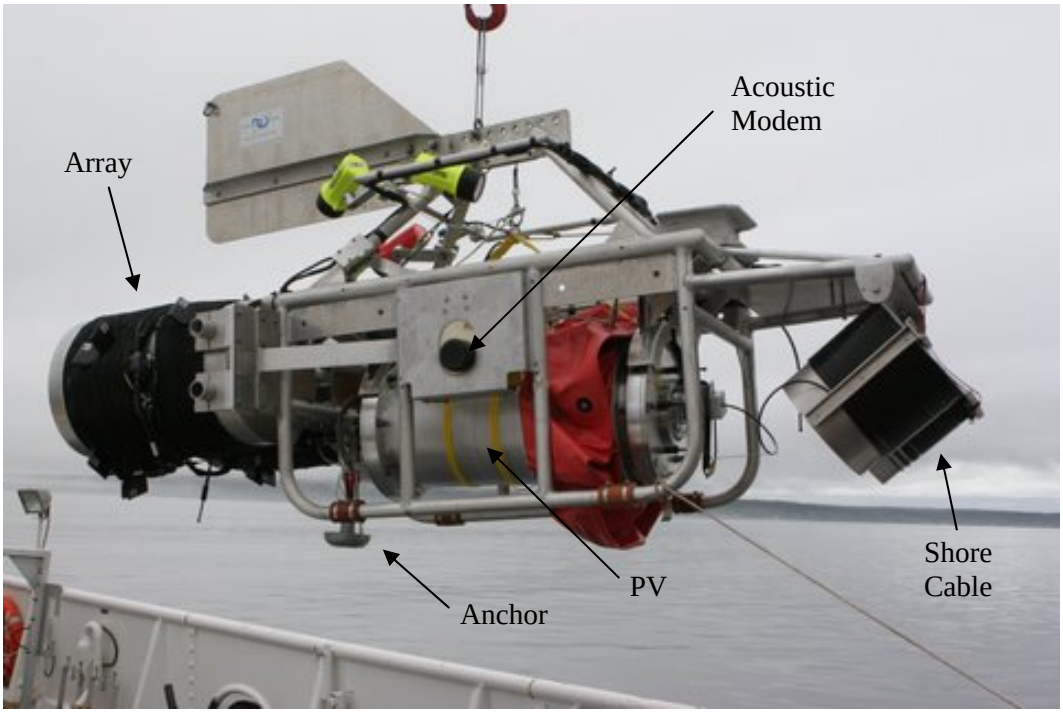

Figure 3. The RDS array deployment sled.

Figure 4. The authors deploying light bulbs with a "down rigger".

be deployed. The light bulb is placed in a holder and lowered to depth by a “down rigger”. For the trial described here, that depth was nominally 40 m. The exact depth is recorded by a self contained recorder attached to the bottom of the bulb holder. When the bulb is at depth, it is broken by dropping a “messenger” down the attached wire. At the exact time of the messenger impact, the GPS position of the boat, and hence, the bulb and the time of the bulb implosion are recorded.

Figure 5 shows the results of the first two steps for the localization of HLA2. During the array deployment, the deployment sled tow-ship traveled along the track shown by the black curve of the figure. This track was chosen in order to lay the array in a curved shape. This shape is preferred to that of a straight line because it helps the RDS source localization algorithms to resolve the left-right source angle ambiguity. At the start of the track, the array anchor was dropped at 44° 33.486´N, 64° 0.383´W. At the end of the track, the PV was dropped at 44° 33.383´N, 64° 0.290´W. These two positions alone were used to determine the lay-down

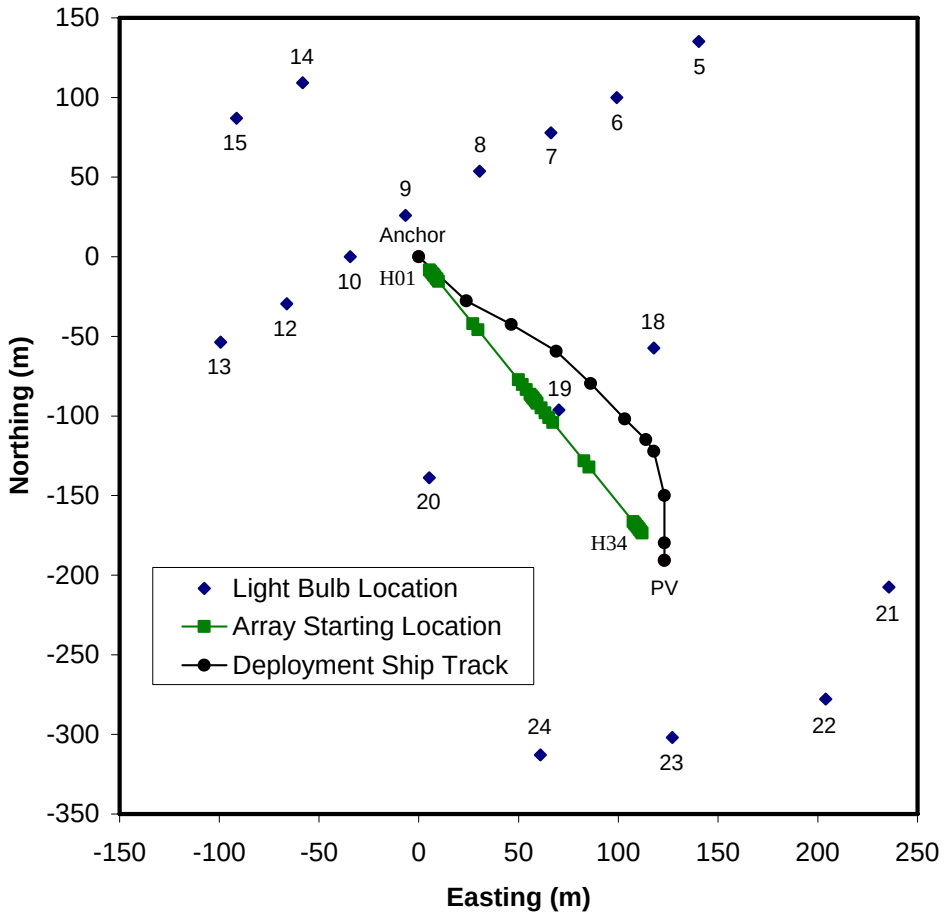

Figure 5. The AEL configuration showing the light bulb source starting locations (dark blue points), the track of the array deployment ship (black curve), and the deployed HLA2 array starting locations (green curve).

direction of the array. Using the position of the anchor as the origin of an X–Y (Easting – Northing) coordinate system, the hydrophone spacings of Fig. 2 were used to calculate the X–Y positions of the individual hydrophones. The green curve of Fig. 5 shows these initial hydrophone locations. In the AEL terminology, these points are referred to as the *Array Starting Locations*. Experience has shown that using a straight starting array is quite sufficient for starting the AEL inversion process. In the second localization step, seventeen light bulbs were imploded around HLA2 at ranges up to about 200 m. Figure 5 shows their locations (dark blue points) and GPS waypoint numbers. These are referred to as the *Source Starting Locations*.

During the light bulb deployment interval, it is necessary to measure the sound speed in the water column. This measured sound-speed profile will be needed by the Rayfast propagation model in the AEL routine to find the eigenrays between the light bulb sources and the hydrophones. Figure 6 shows the sound speed profile that was measured during the light bulb deployment around HLA2. The profile is downward refracting with an average speed of 1460.60 m/s in the water column.

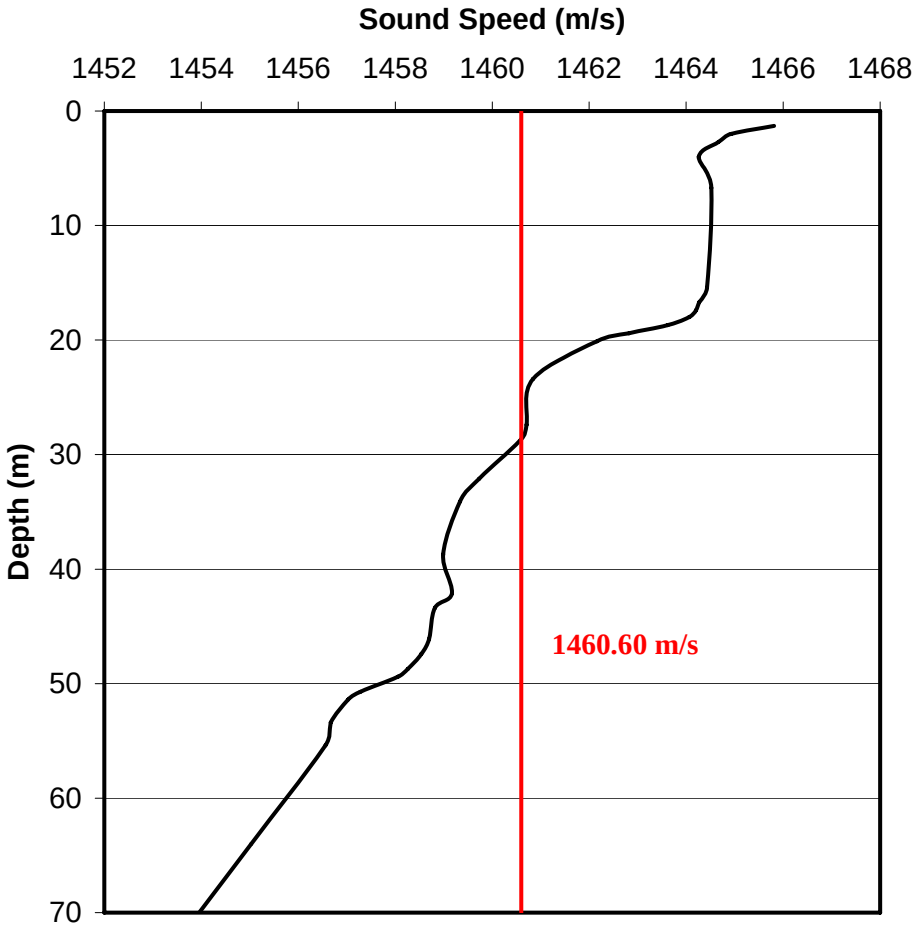

Figure 6. The AEL sound speed profile.

4. Array Localization Results

The third step in the AEL process is the detection and processing of the light bulb signatures recorded by the hydrophones of the array. As stated in the last section, for most of the RDS trials, this step was always done after the array was recovered. However, during the demonstration trial, this step was carried out for HLA2 in an autonomous mode using a C++ code compiled on the array "algorithm board" located in the PV. The results of this AEL pre-processing were then transmitted to *CFAV Quest* using an RF link.

4.1 Autonomous Light Bulb Pre-Processing

The autonomous AEL pre-processing code carries out two tasks. First, it locates the light bulb signatures within the data file. Second, it processes each signature to find the arrival time of the direct arrival at each hydrophone.

Figure 7 shows a flow diagram for the first task. The grey boxes represent the data handling, the yellow boxes represent the data processing, and the blue boxes represent the decision process. The pre-processing is initiated from the operator station using a Graphical User Interface (GUI) format and can run much faster than real time when processing the AEL light bulb file. As per the flow diagram of the figure, two channels of data are extracted from the bulb file. These two channels usually correspond to hydrophones H01 and H34, the two sensors with the largest separation in space and, hence, time delay. These data are then filtered to the frequency range of a light bulb signature. From this point onward, the data are processed in groups of 100 points that advance one point at a time. With a sampling rate of 2000 Hz, this corresponds to 50 ms of data that advances in steps of 0.5 ms. For each 100-point group, two averages are calculated, one over the whole 100 points, and one over the last 3 points (points 98 to 100). The ratio of the short average to the long average is then compared to a threshold. If it exceeds the threshold (29 for the pre-processing of the HLA2 data), a possible light bulb signature has been found. If not, the 100-point group is advanced by one point and the averaging process is repeated. In order to distinguish between the onset of a new light bulb signature and the tail end of the last signature, a possible signature is only accepted if it is separated from the last by at least 500 points (0.25 s). In addition, in order to make sure that a possible signature is not just a random impulse in the data stream, a check is made to make sure that it occurs on both channels at the same time. If all of the above three tests are passed successfully, then the possible signature is deemed a true light bulb signature and its position within the file is recorded for the next task. This procedure is repeated until all the light bulb signatures have been found.

Once the file positions of all the light bulb signatures have been recorded, the pre-processing continues with the second task, that is, the calculation of the direct arrival times. A flow diagram for this task is shown in Fig. 8. As before, the grey boxes represent the data handling, the yellow boxes represent the data processing, and the blue box represents the decision process. Using the light bulb file position, the bulb signature for each of the 34 channels is extracted from the data file. Each channel data segment is 8192 points long (4.096 s) and is centered on the bulb file position. Once again, the data must be filtered to the desired frequency range. The processing begins by normalizing the signature data. As an example, Fig. 9(a) shows the normalized signature for light bulb number 5 (see Fig. 5) as recorded on hydrophone H01. As indicated by the figure, the important portion of the signature is contained within the first 0.15 s (300 points).

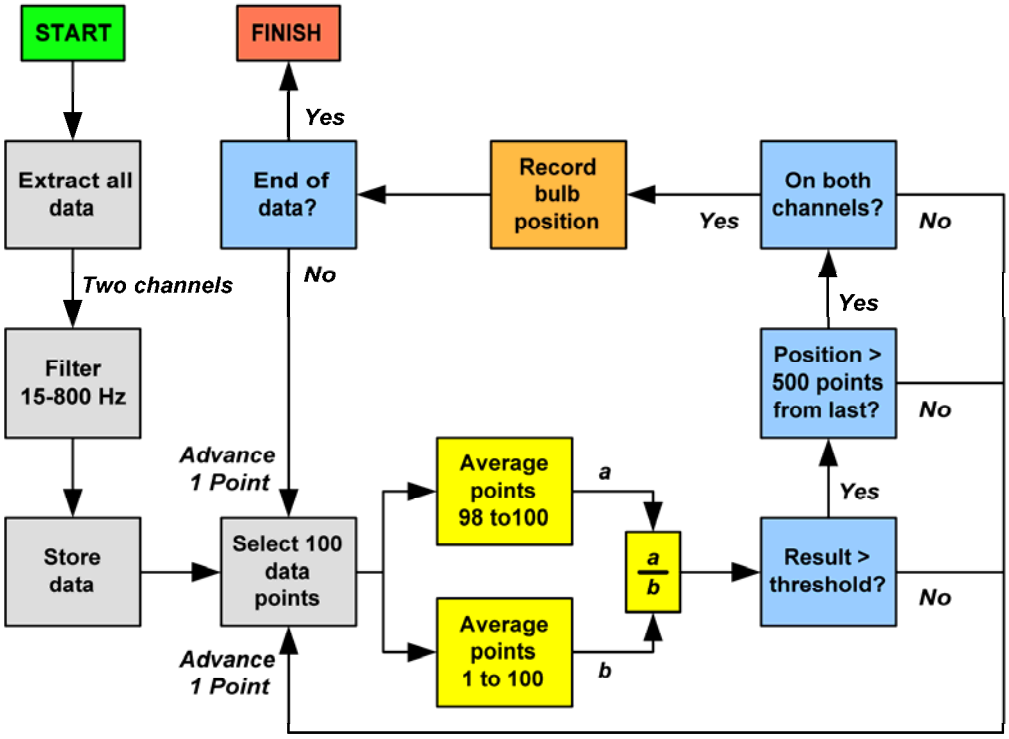

Figure 7. Flow diagram for the light bulb file position search.

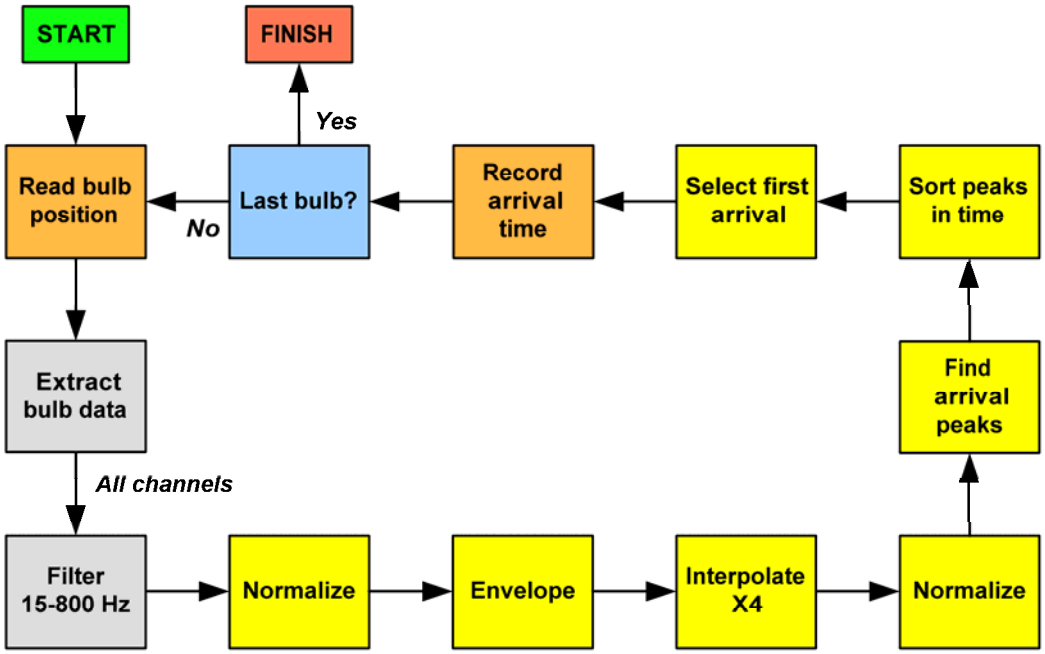

Figure 8. Flow diagram for the direct arrival time calculation.

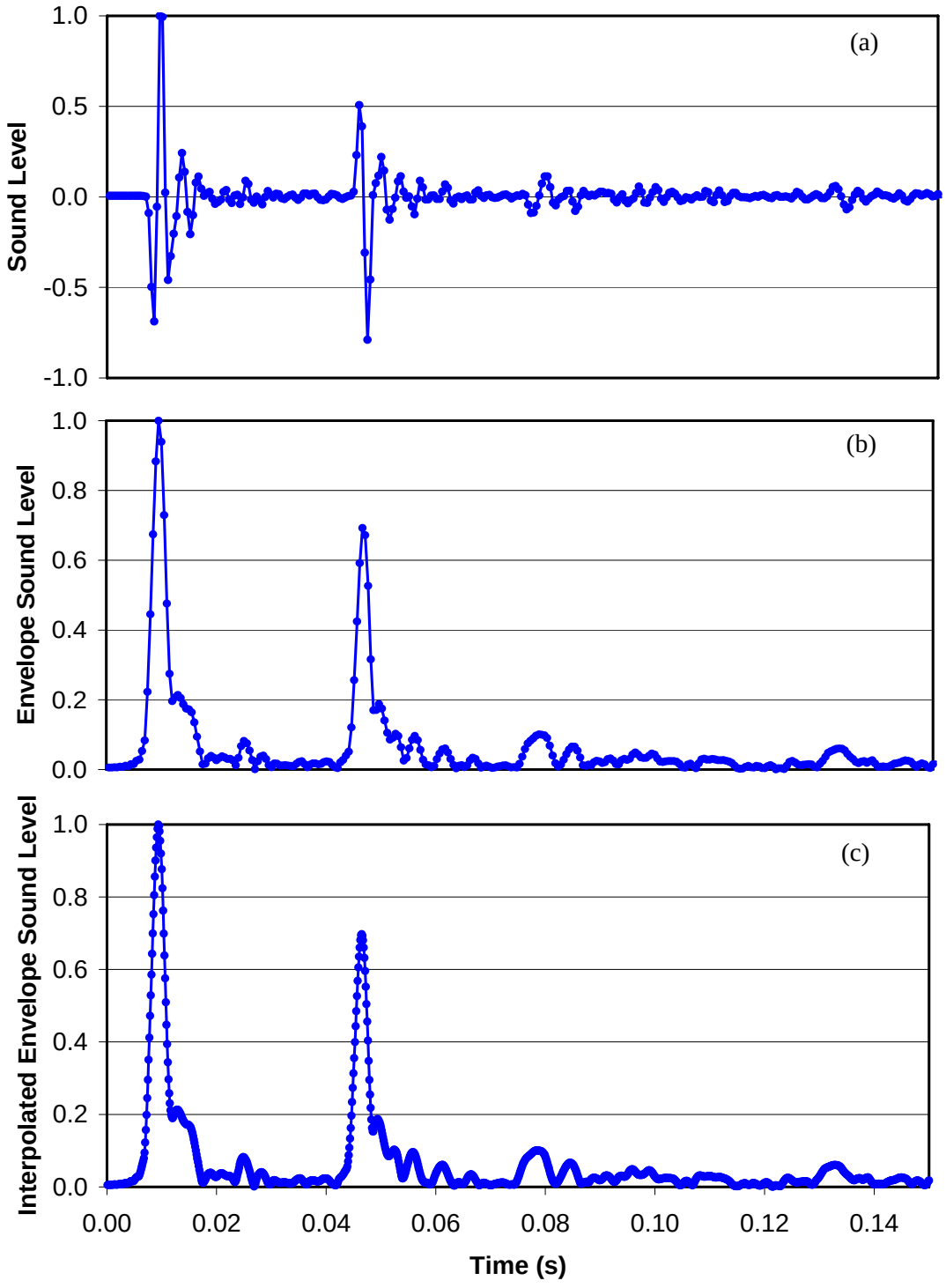

Figure 9. The time domain signature for light bulb number 5 as recorded on hydrophone H01, (a) recorded time series, (b) envelope of the time series, and (c) interpolated envelope.

At least three arrivals are clearly visible. They are, in order of arrival time, the direct arrival, the surface reflected arrival, and one of the first bottom-bounce arrivals. However, because of the bubble pulse oscillations from the bulb implosion [8], the arrival times are difficult to determine. To alleviate this problem, a Hilbert transform is used to compute the envelope of the signature. As shown in Fig. 9(b), this emphasizes the power in each of the arrivals. Finally, the signature is interpolated by a factor of four to increase the accuracy of the arrival times to with 0.125 ms and then re-normalized. Figure 9(c) shows the final result for the example. To finish the task, a peak picking routine is used to find the arrivals. Since the direct arrival is not always the largest arrival, the peaks are sorted in arrival time so the time corresponding to the direct arrival can be determined and recorded for each channel. It should be noted that this arrival time is relative to the start of the extracted data segment. However, this is sufficient to determine the direct arrival delay times along the array. This procedure is repeated until all the light bulb signatures have been processed.

When the pre-processing is complete, two files are sent to the operator station via the RF link. The first file contains the direct arrival time for each hydrophone-bulb pair. The second file contains the absolute time of each light bulb implosion. These latter times are needed to match each light bulb in the data file to a light bulb in the GPS file that was made during the bulb deployment exercise.

Once the operator station has the AEL pre-processing files, the operator needs to determine if the arrival time files have been processed correctly. The easiest way of doing this is to compute a plot for each light bulb that shows the delay time along the array as a function of hydrophone position. The time delay is simply the difference between the arrival time at a hydrophone and the arrival time at the reference hydrophone. For HLA2, the reference was hydrophone H01. Correspondingly, the hydrophone position is the distance of the hydrophone from the reference hydrophone.

As an example, the black curve of Fig. 10 shows the time delay plot corresponding to light bulb number 5 as received with HLA2. Note the smooth shape of the time delay curve. This indicates that the arrival times have been determined correctly. Also note that the time delays are all positive. This indicates that the position of the bulb implosion was closer to hydrophone 1 than to the other hydrophones. Any abnormalities or sudden jumps in the shape of this curve would indicate errors in the data. The red and green curves in the figure are the maximum and minimum time delay curves, respectively, that are possible with HLA2. These boundaries are based on the hydrophone spacings and the average sound speed in the water near the array (see Fig. 6). Any results outside these boundaries would also indicate errors in the data.

4.2 Array Localization

The four key inputs are now in place to carry out the AEL localization of the array. First, the array starting location on an X–Y coordinate system has been determined. The Z coordinate, depth, is the same as the bottom depth. For HLA2 that depth was 68.9 m. Second, the source starting locations are known on the same coordinate system. For HLA2, the light bulb depth recorder failed, so a nominal source depth of 40 m was used. Third, the sound speed profile was measured during the time of the light bulb deployment. Finally, fourth, the direct arrival times along the array have been measured for each light bulb and matched to a light bulb location.

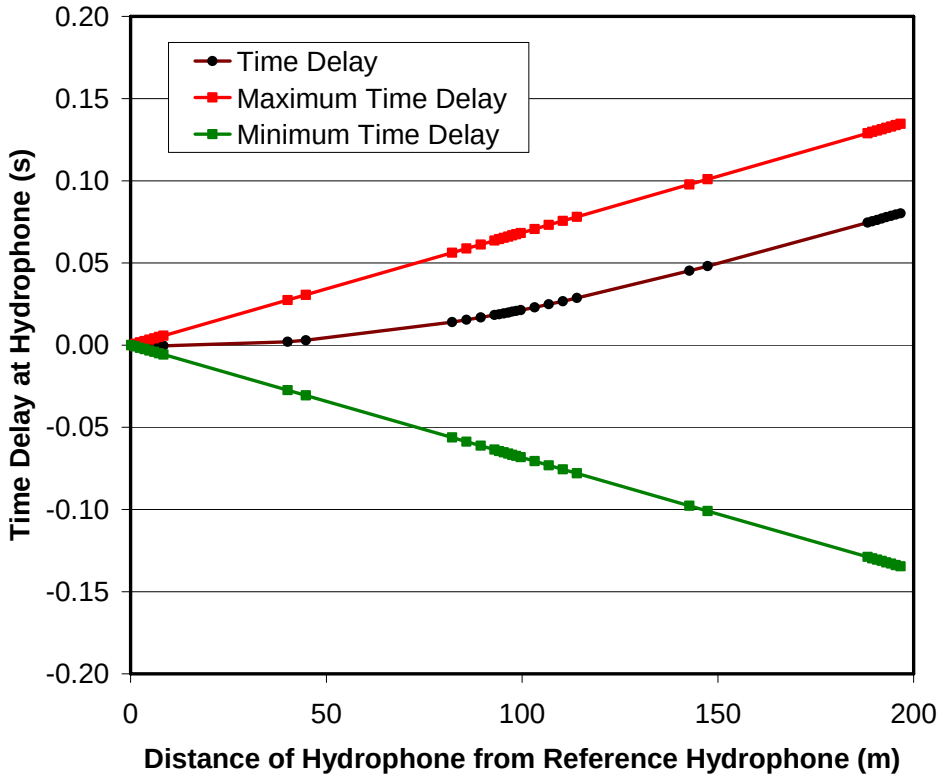

Figure 10. The time delay due to light bulb number 5 as measured with respect to hydrophone H01 at each hydrophone of the localized array (black curve). The red and green curves are the maximum and minimum time delay curves, respectively, that are possible with the localized array.

The AEL procedure requires estimates of the uncertainties of the input source and receiver positions. For HLA2, it was assumed that the standard deviations of the hydrophone positions were 150 m in northing (Y direction) and easting (X direction) and 2 m in depth (Z direction). Also, the standard deviations for the source positions were assumed to be 5 m in northing and easting and 2 m in depth. Finally, the uncertainties in the time delays resulting from the source impulses as measured with the array were assumed to be 0.1 ms.

The control parameters for the AEL inversion of HLA2 are shown in Table 1. The first eight parameters are straight forward. The number of sources, **ns**, and the number of hydrophones, **nh**, were 17 and 34, respectively. Since the data was real, the simulation switch, **isim**, was turned off (isim=0). The array was deployed in a smooth line, so the smooth regulation switch, **ismooth**, was turned on (ismooth=1). As discussed in Section 1, the array was localized using the direct path arrivals from non-synchronized light-bulb sources. Hence, the number of ray paths, **npath**, was set to 1, the character of that path was "d" for direct, and the source instant identifier, **it0**, was set to 1 for unknown. Lastly, the χ^2 fit to the data that must be reached to achieve convergence, **chi_final**, was set to the product of the numbers of the sources, receivers and paths, that is, $N_h \times N_s \times N_p = 34 \times 17 \times 1 = 578$ (a setting of -1 selects this value as the default). The next six parameters take some AEL inversion experience to set. The maximum change in hydrophone location between iterations, **delta_m**, was set to a value of 0.1 m. In all of the RDS

Table 1. Inversion input parameters for the localization of HLA2.

Parameter	Value	Description
ns	17	Number of sources.
nh	34	Number of hydrophones.
isim	0	Simulation switch: isim=0 to read measured data, isim=1 to simulate data.
ismooth	1	Smooth regulation switch: ismooth=0 for not a smooth array, ismooth=1 for a smooth array.
npath	1	Number of acoustic ray paths in the data.
	d	Character of the ray path: d for direct, s for surface, b for bottom, sb for surface-bottom, etc.
it0	1	Source instant identifier: it0=0 for known, it0=1 for unknown.
chi_final	-1	Final required χ^2 fit to the data: negative value gives the default of (ns nh npath), t he number of data.
delta_m	0.1 m	Maximum average 3D hydrophone location change between iterations permitted at convergence.
niter	100	Maximum number of iterations for the inversion.
chi_reduce	2.0	Factor to reduce the χ^2 misfit by at each iteration.
fact	1.0	Parameter controlling the relative trade-off between fitting prior source and receiver location estimates and achieving minimal curvature (only used when ismooth=1).
mu	10000.	Starting value for the trade-off between fitting the data and fitting the prior estimates.
r_tol	0.05 m	Range tolerance for ray-tracing convergence.
wdep_err	0.0 m	Approximate uncertainty in water-column depth (0.0 m if no bottom-reflected arrivals included).
c_err	1.0 m/s	Approximate uncertainty in water-column sound speed due to bias error.
iseed	3555	Random seed for simulation mode which is used to add Guassian random errors to data and prior estimates (only used when isim=1).

localization cases, this value has worked well. The maximum number of iterations that are allowed for the AEL problem, **niter**, was set conservatively large at 100. Most of the RDS AEL problems have converged in 20 iterations or less. For "easy" AEL inverse problems, the factor to reduce the χ^2 misfit by at each iteration, **chi_reduce**, can be large (for example, a factor of 100) for fast convergence. However, for "difficult" inversions like the one presented here, a small reduction of 2 ensures convergence. The parameter that controls the relative trade-off between fitting the prior source and receiver location estimates and achieving a solution with minimal array curvature, **fact**, is only used when the smoothing switch is on. This parameter is equivalent to the ratio μ_2 / u_1, where μ_1 and μ_2 are as in (6). For all of the RDS inversion problems, an equal trade-off (fact=1.0) was found to be effective. The starting value for the trade-off between fitting the data and fitting the prior estimates, **mu**, was set conservatively large at 10,000. Generally, values of between 1000 and 10,000 are used. The range tolerance for the convergence

of the raytracings, **r_tol**, is usually chosen to be somewhere between 0.05 and 0.1 m. A value of 0.05 m was found to be effective for the acoustic environment of St. Margaret's Bay. Only one of the last three parameters of Table 1 is important for the localization of HLA2. The uncertainty in the water-column sound speed due to bias errors, **c_err**, was estimated to be approximately 1.0 m/s. This value has been used for all of the AEL inversions in St. Margaret's Bay. The uncertainty in the water-column depth, **wdep_err**, was not needed (set to zero) because bottom-reflected arrivals were not used for the this inversion. Likewise, the random seed number, **iseed**, is only used for simulated cases.

Table 2 shows the output of the AEL algorithm during the localization of the HLA2 array. The **iter** value is the number of iterations for the inversion. The **chi** value is the χ^2 non-linear data misfit and the **chi_lin** value is the χ^2 linear data misfit. The **chi_targ** value is the data misfit that is the target for that iteration. The **chim** value is the normalized χ^2 data misfit for the prior estimates of the source and receiver positions. The **chis** value is the array smoothness, that is, a value that is representative of the amount of array curvature required by the inversion. The **delta** value is the RMS change in hydrophone positions between iterations. Finally, the **mu** value is the trade-off between fitting the data and fitting the prior estimates. As shown in the table, the inversion for HLA2 converged in just 17 iterations. The algorithm stopped when the two criteria of Section 2.3 where met. First, the χ^2 non-linear data misfit (**chi**) was reduced to the final target value (**chi_final** of Table 1) that was specified at input, that is, $N_h \times N_s \times N_p = 34 \times 17 \times 1 = 578$. Second, the RMS change in the receiver positions between iterations (**delta**) was reduced to

Table 2. Inversion output varables for the localization of HLA2.

iter	chi	chi_lin	chi_targ	chim	chis	delta	mu
0	6791737.9			0.00000000	3.3212375e-008		
1	2712659.5	2805615.3	3395869.0	0.00000000	3.7445397e-006	9.4397601	1000000.
2	1617702.8	1648308.9	1356329.7	0.026874076	6.1635491e-006	4.6039139	421697.
3	704162.49	730942.61	808851.42	0.048192673	6.0602662e-006	4.7975013	177828.
4	215403.79	229937.70	352081.24	0.072656266	9.2382522e-006	4.2517804	74989.4
5	164577.48	165388.17	107701.90	0.092009107	1.0632748e-005	0.87659809	64938.2
6	131113.48	131275.71	82288.738	0.092441014	1.1498495e-005	0.56047540	56234.1
7	105496.75	105582.99	65556.742	0.095076701	1.2366880e-005	0.48643545	48696.8
8	85020.287	85077.211	52748.373	0.097976407	1.3351821e-005	0.44522782	42169.6
9	68601.951	68638.567	42510.144	0.10097409	1.4492471e-005	0.41131380	36517.4
10	55452.367	55478.583	34300.975	0.10405893	1.5795454e-005	0.37915315	31622.8
11	16761.476	16907.071	27726.183	0.10725530	2.7562713e-005	1.6499752	13335.2
12	5890.1996	5913.2856	8380.7382	0.13032566	5.0282756e-005	0.94377368	5623.41
13	2487.0072	2490.3561	2945.0998	0.15928203	9.7341269e-005	0.52970020	2371.37
14	1311.4836	1311.7335	1243.5036	0.18835081	0.00019385594	0.33014191	1000.00
15	789.76788	789.36901	655.74182	0.21297471	0.00038281633	0.23676881	421.696
16	577.92892	577.48175	578.000	0.23790695	0.00060310177	0.13354628	240.79327
17	578.71750	578.70861	578.000	0.25786010	0.00060356004	0.0049534711	240.79327

a value smaller than the target value (**delta_m** of Table 1) that was specified at input, that is, 0.1 m. Notice that as **chi** decreased, **chim**, the χ^2 data misfit for the prior estimates of the source and receiver positions, increased from zero as expected. Also notice that the **chis** value increased with the number of iterations. That is, the array shape changed from the starting shape of a straight line to the final shape of a smooth curve.

The final array position in northing and easting that was obtained from the AEL inversion of HLA2 is shown by the red curve in Fig. 11. As indicated by the figure, the array was deployed in a slight "S" shape with average offsets from the starting location (green curve) of 35.7 m in northing and -20.2 m in easting. These offsets are believed to be due to the offset between the deployment sled and the GPS antenna on the sled tow-ship, which could be as much as 60 m, as well as the errors in the GPS measurements themselves. To investigate this further, the tow-ship track of Fig. 5 (black curve), with the exception of the points corresponding to the anchor and PV, was used in conjunction with a 60-m offset between the deployment sled and the tow-ship to estimate the track of the sled during the array deployment. This estimated track is shown by the

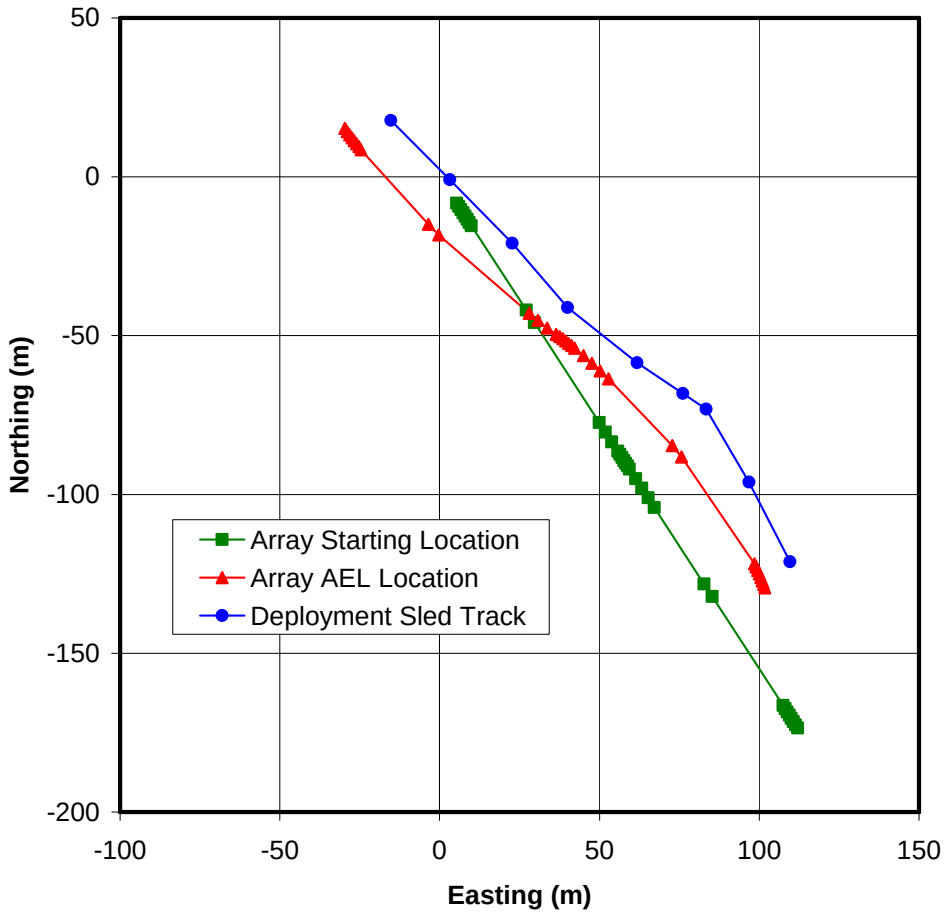

Figure 11. The AEL results showing the starting array (green curve), the track of the array deployment sled (blue curve), and the localized HLA2 array (red curve).

blue curve of Fig. 11. Clearly, the result of the AEL inversion yields an array shape that very much mirrors the track of the sled with average offsets of only -5.4 m in northing and -11.2 m in easting. This close comparison in shape shows that the AEL process has yielded an accurate result for HLA2. In Fig. 12, the red curve shows the hydrophone depths of the localized array. They range between 68.5 and 69.1 m with only a very small average offset of -0.04 m from the starting depth (green curve).

It should be noted that the hydrophone separations along HLA2 are fixed to the values that are shown by the array diagram of Fig. 2. Therefore, during a normal deployment, the spacing between any two hydrophones can never be greater than their fixed separation. The present version of the AEL algorithm does not take this spacing restriction into account. Therefore, a good measure of the AEL accuracy is how close the localized hydrophone separations are to the starting separations. Figure 13 shows a plot of the difference between these two separations. That is, for adjacent hydrophone pairs, it shows a plot of the localized separation minus the starting separation. For a perfect localization, this difference would never be a positive number. As shown in the figure, the worst case was a difference of +0.233 m for hydrophones 24 and 25. However, the average difference across the array was only +0.01 m. This small difference boosts the confidence level of the AEL solution.

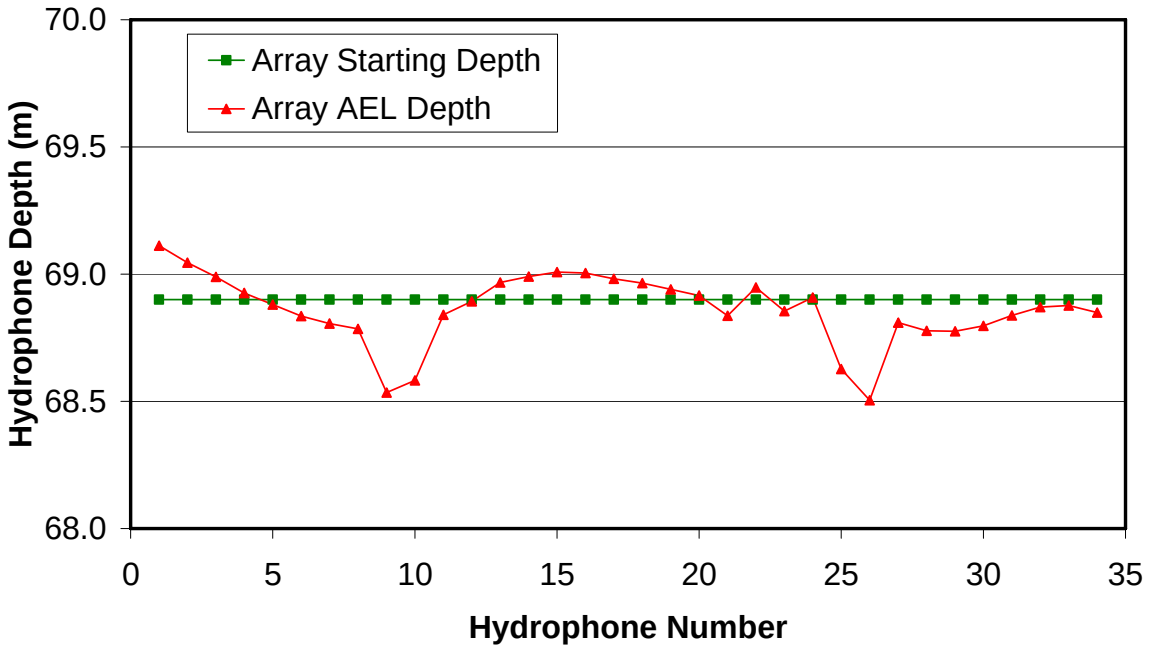

Figure 12. The hydrophone depths for HLA2 showing the starting array depths (green curve) and the localized array depths (red curve).

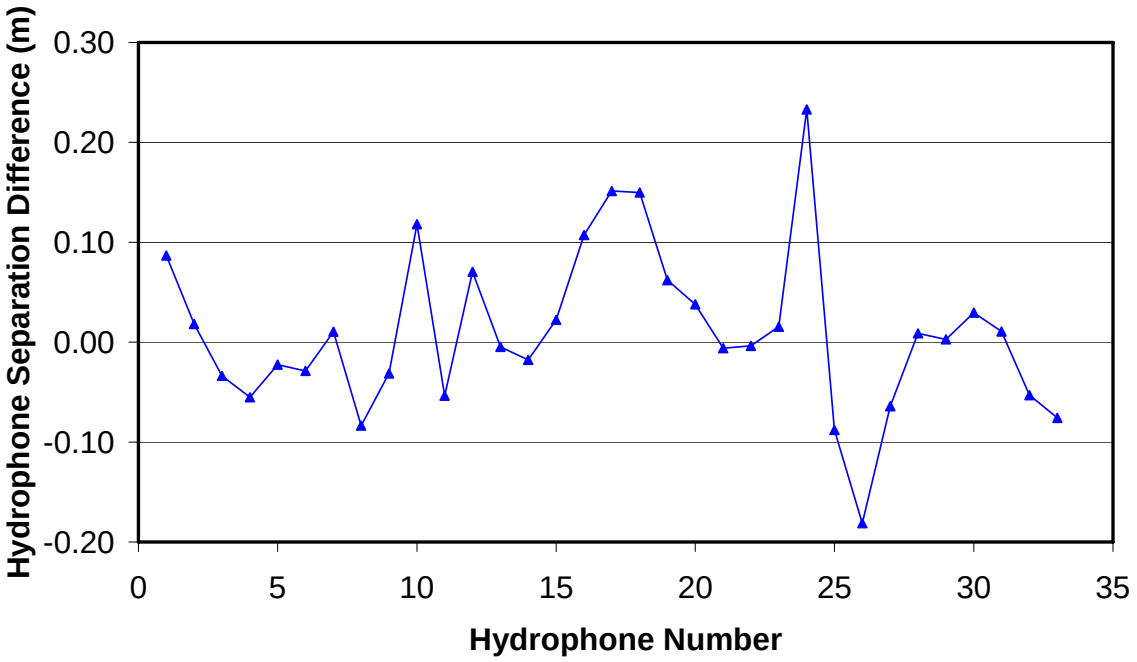

Figure 13. The difference in the separation of adjacent HLA2 hydrophones of the localized array from that of the starting array.

4.3 Monte Carlo Error Analysis

An important aspect of the AEL inversion problem is estimating the uncertainty of the regularized solution. For linear problems with Gaussian-distributed data errors and prior estimates, the posterior model covariance matrix that was given in (9) can be used to estimate the linearized uncertainty estimates for the solution in the form of standard deviations. Figure 14(a) shows the uncertainty estimates for the localization of HLA2 in easting (red curve), northing (green curve) and depth (blue curve). The black curve is the resultant of the three directions. As the figure shows, the uncertainty in the solution is less than 1.7 m for the easting and northing and less than 0.8 m for the depth.

Alternatively, a Monte Carlo analysis of the regularized solution can provide more exact uncertainty estimates, but at a much higher computational expense. In this analysis, the AEL localized source and hydrophone positions are assumed to define the true positions for a synthetic inverse problem, and the acoustic arrival time data are simulated with the Rayfast model. A large number of independent inversions are then carried out, each with different random errors applied to the arrival times and to the starting location estimates. The standard deviations about the true hydrophone positions can then be computed from the ensemble of inversion results.

A Monte Carlo uncertainty analysis was carried out using the regularized solution for HLA2 that was described in Section 4.2. A total of 100 AEL inversions were used in all. The resulting estimate for the absolute error in the regularized solution is shown in Fig. 14(b). Once again, the red curve is the error in easting, the green curve is the error in northing, the blue curve is the error

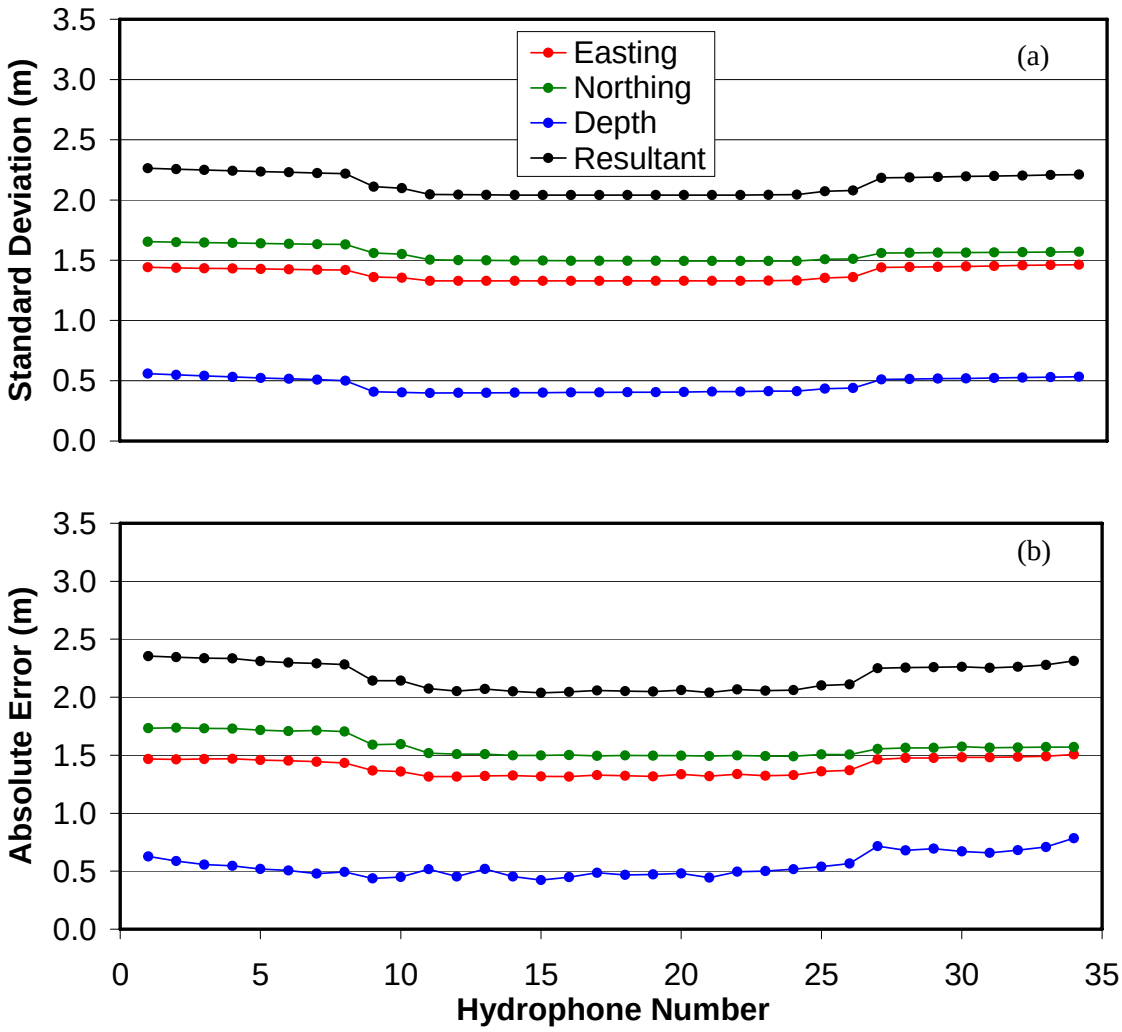

Figure 14. (a) The AEL standard deviations of each hydrophone position of the localized array for HLA2 in easting (red curve), northing (green curve), and depth (blue curve). The black curve is the resultant of the three directions. (b) The absolute error in the same format as computed by the Monte Carlo uncertainty analysis.

in depth, and the black curve is the resultant of the three directions. If the results of this figure are compared to those of Fig. 14(a), it is clear that the Monte-Carlo absolute errors are in very good agreement with the uncertainty estimates obtained by the AEL inversion.

One of the benefits of the Monte Carlo uncertainty analysis is that it can remove the effects of translation and rotation between the starting array and the localized array. What is left is the uncertainty in the shape of the array, that is, the relative error between hydrophones. Figure 15 shows the relative error for the analysis of HLA2 in the same format as the previous figure. These errors are very small; less than 0.75 m for all hydrophones. In particular, near the center of the array, that is, in the middle of the "S" curve, the errors are less than 0.3 m. The relative error is important in that the accuracy of most source localization algorithms depends on the relative

positions (spacings) of the hydrophones and less so on the global positions. This error analysis supports the hydrophone-separation-difference results that were shown in Fig. 13.

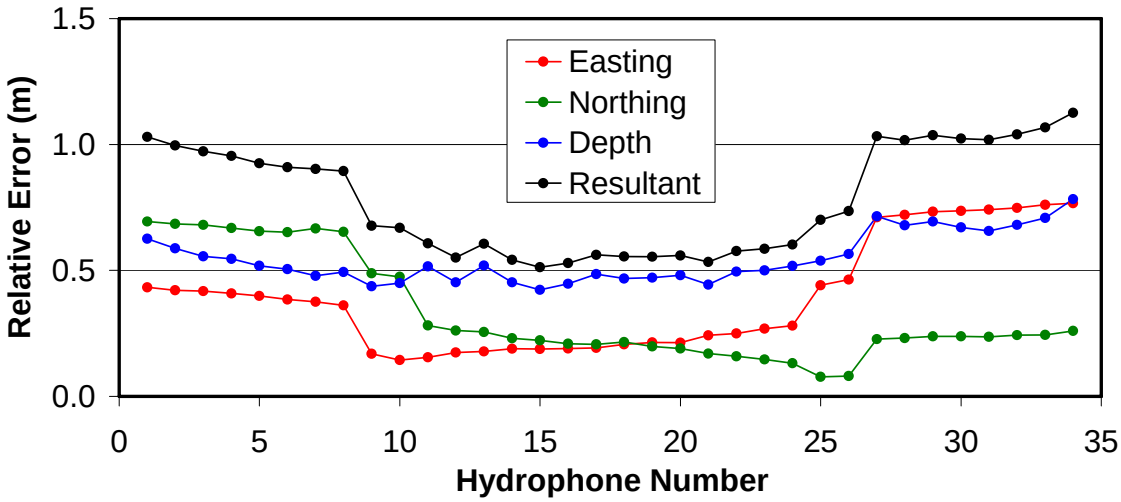

Figure 15. The relative errors of each hydrophone position of the localized array for HLA2 in easting (red curve), northing (green curve), and depth (blue curve) as computed by the Monte Carlo uncertainty analysis. The black curve is the resultant of the three directions.

5. Conclusions

This paper describes and demonstrates an AEL inversion process for localizing the hydrophones of a RDS array. The inversion produces an estimate of the 3D positions for the array hydrophones and impulsive sources included in the localization process. It is based on the linearized inversion of the measured arrival time data from the sources and uses the method of regularization to include *a priori* information such as the approximate positions of the sources and hydrophones. That is, the inversion is set up to achieve a misfit to the data that is statistically consistent with the estimated uncertainties of this data, while applying additional independent prior information about the solution to the inversion.

The AEL demonstration makes use of imploding light bulbs at depth as a convenient source of impulsive acoustic energy. This is not a suggested method for an operationally deployed array system. An operational array would be localized using the same theory, but the sound source would be quite different. For example, during the RDS project, experiments were carried out to test a prototype AEL method that used of an AUV carrying a compact, low-frequency impulsive sound source to conduct AEL operations in a more clandestine manner.

There are four key inputs that are required to carry out the AEL localization of an array. First, the array starting location on an X–Y–Z (Easting–Northing–Depth) coordinate system has to be determined. Second, the source starting locations must be known on the same coordinate system. Third, the sound speed profile has to be measured during the time of the light bulb deployment. Finally, fourth, the direct arrival times along the array have to be measured for each light bulb and then matched to a light bulb location.

An AEL preprocessing algorithm was described that is effective in locating the signature of a light bulb implosion in an RDS data file and can determine the absolute implosion time as well as the direct arrival time at each hydrophone in the array. Because this algorithm is fully autonomous, all the data that is required for a full localization of the array can be obtained while the array is still deployed. This relatively small amount of data is sent to a remote operator station via a RF link so that the AEL inversion can be carried out.

To demonstrate the overall AEL process, the algorithm was used to localize the sensors of a horizontal array denoted as HLA2 during the RDS demonstration trial. The results indicated that the array was deployed in a slight “S” shape with average offsets from the starting location of 35.7 m in northing and -20.2 m in easting. These offsets were due to the offset between the array deployment sled and the GPS antenna on the sled tow-ship, which could be as much as 60 m, as well as the errors in the GPS measurements themselves. Further investigation revealed that the results of the AEL inversion yielded an array shape that very much mirrored the track of the deployment sled with average offsets of only -5.4 m in northing and -11.2 m in easting. This close comparison in shape demonstrated that the AEL process yielded an accurate result for HLA2.

An important aspect of the AEL inversion problem is estimating the uncertainty of the regularized solution. For linear problems with Gaussian-distributed data errors and prior estimates, the posterior model covariance matrix can be used to estimate the linearized uncertainty estimates for the solution in the form of standard deviations. Alternatively, a Monte Carlo analysis of the

regularized solution can provide more exact uncertainty estimates, but at a much higher computational expense. It was found that the uncertainty in the solution for HLA2 was less than 1.7 m for the easting and northing and less than 0.8 m for the depth. In addition, the relative errors between the hydrophones of HLA2 were found to be very small; less than 0.75 m for all hydrophones and less than 0.3 m near the center of the array. It is these relative errors that are of primary importance for array beamforming and relative source localization.

In summary, this paper has shown that AEL is a fast and effective algorithm for localizing the hydrophones of the RDS horizontal arrays.

6. References

1. C. Somers, T. Kennedy and J. McInnis, “Rapid Deployable Systems (RDS) for Underwater Surveillance: Final Report,” DRDC Atlantic CR 2006-223, November 2006.

2. J. Kennedy, A. Proctor, E. Gamroth, C. Bradley, and G.J. Heard, “Decoupled modelling and controller design for the autonomous underwater vehicle: MACO,” International Journal of the Society for Underwater Technology, Vol. 27, No. 1, pp. 11-21, 2007.

3. S.E. Dosso, G.H. Brooke, S.J. Kilistoff, B.J. Sotirin, V.K. McDonald, M.R. Fallat and N.E. Collision, “High-precision array element localization of vertical line arrays in the Arctic Ocean,” IEEE J. Oceanic Eng., **23**, 365–379 (1998).

4. S.E. Dosso, M.R. Fallat, B.J. Sotirin and J.L. Newton, “Array element localization for horizontal arrays via Occam’s inversion,” J. Acoust. Soc. Am. **104**, 846–859 (1998).

5. S.E. Dosso and G.R. Ebbeson, “Array Element Localization Software Upgrade,” DRDC Atlantic CR 2005-242, September 2005.

6. S.E. Dosso and G.R. Ebbeson, “Array Element Localization Accuracy and Survey Design,” Can. Acoust., Vol. 34, No. 4, 3-13 (2006), also DRDC Atlantic SL 2005-241, December 2006.

7. S.E. Dosso, N.E. Collison, G.J. Heard and R.I. Verrall, “Experimental validation of regularized array element localization,” J. Acoust. Soc. Am. **115**, 2129–2137 (2004).

8. G.J. Heard, M. McDonald, N.R. Chapman and L. Jaschke, “Underwater Light Bulb Implosions: A Useful Acoustic Source,” Proc. IEEE Oceans ’97, 8 pages (1997).

List of symbols/abbreviations/acronyms/initialisms

3D	Three Dimensional
AEL	Array Element Localization
AUV	Autonomous Underwater Vehicle
DRDC	Defence Research and Development Canada
GPS	Global Positioning System
GUI	Graphical User Interface
HLA	Horizontal Line Array
MDA	MacDonald Dettwiler and Associates
PV	Pressure Vessel
RDS	Rapidly Deployable System
RF	Radio Frequency
TDP	Technical Demonstration Project
UEP	Underwater Electric Potential
VLA	Vertical Line Array

Distribution list

INTERNAL

Library (5)

Gordon Ebbeson (1)

Garry Heard (1)

Francine Desharnais (1)

David Hazen (1)

Neil Sponagle (1)

Nicole Collison (1)

Total Internal – 11

EXTERNAL

DRDKIM (1)
NDHQ

Marie-Noël R. Matthews (1)
Department of Oceanography
Dalhousie University
3rd Floor, Life Sciences Centre
1355 Oxford St.
Halifax, NS B3H 4J1

Stan Dosso (1)
School of Earth and Ocean Sciences
University of Victoria,
Victoria, BC V8W 3P6

Total External – 3

Total copies required – 14

This page intentionally left blank.

DOCUMENT CONTROL DATA

(Security classification of title, body of abstract and indexing annotation must be entered when the overall document is classified)

1. ORIGINATOR (the name and address of the organization preparing the document. Organizations for whom the document was prepared, e.g. Centre sponsoring a contractor's report, or tasking agency, are entered in section 8.)

DRDC Atlantic

2. SECURITY CLASSIFICATION (overall security classification of the document including special warning terms if applicable).

UNCLASSIFIED

3. TITLE (the complete document title as indicated on the title page. Its classification should be indicated by the appropriate abbreviation (S,C,R or U) in parentheses after the title).

Array Element Localization of a Rapidly Deployable System of Sensors

4. AUTHORS (Last name, first name, middle initial. If military, show rank, e.g. Doe, Maj. John E.)

Ebbeson, Gordon R., Heard, Garry J., Desharnais, F., Matthews, Marie N.R. and Dosso, Stan E.

5. DATE OF PUBLICATION (month and year of publication of document)	6a. NO. OF PAGES (total containing information Include Annexes, Appendices, etc).	6b. NO. OF REFS (total cited in document)
August 2007	27 (approx.)	8

7. DESCRIPTIVE NOTES (the category of the document, e.g. technical report, technical note or memorandum. If appropriate, enter the type of report, e.g. interim, progress, summary, annual or final. Give the inclusive dates when a specific reporting period is covered).

TECHNICAL MEMORANDUM

8. SPONSORING ACTIVITY (the name of the department project office or laboratory sponsoring the research and development. Include address).

Defence R&D Canada – Atlantic
PO Box 1012
Dartmouth, NS, Canada B2Y 3Z7

9a. PROJECT OR GRANT NO. (if appropriate, the applicable research and development project or grant number under which the document was written. Please specify whether project or grant).	9b. CONTRACT NO. (if appropriate, the applicable number under which the document was written).
RDS TD	

10a ORIGINATOR'S DOCUMENT NUMBER (the official document number by which the document is identified by the originating activity. This number must be unique to this document.)	10b OTHER DOCUMENT NOs. (Any other numbers which may be assigned this document either by the originator or by the sponsor.)
DRDC Atlantic TM 2007-009	

11. DOCUMENT AVAILABILITY (any limitations on further dissemination of the document, other than those imposed by security classification)

(X) Unlimited distribution
( ) Defence departments and defence contractors; further distribution only as approved
( ) Defence departments and Canadian defence contractors; further distribution only as approved
( ) Government departments and agencies; further distribution only as approved
( ) Defence departments; further distribution only as approved
( ) Other (please specify):

12. DOCUMENT ANNOUNCEMENT (any limitation to the bibliographic announcement of this document. This will normally correspond to the Document Availability (11). However, where further distribution (beyond the audience specified in (11) is possible, a wider announcement audience may be selected).

13. ABSTRACT (a brief and factual summary of the document. It may also appear elsewhere in the body of the document itself. It is highly desirable that the abstract of classified documents be unclassified. Each paragraph of the abstract shall begin with an indication of the security classification of the information in the paragraph (unless the document itself is unclassified) represented as (S), (C), (R), or (U). It is not necessary to include here abstracts in both official languages unless the text is bilingual).

The Rapidly Deployable Systems (RDS) technology demonstration project (TDP) was a major research effort that was conducted by Defence Research and Development Canada (DRDC) – Atlantic. The purpose of this project was to develop a deployable array system with on-board processing components that would be capable of detecting, localizing, and eventually classifying sources of acoustic and electromagnetic energy traveling on or underneath the sea surface. A difficult requirement for the success of the RDS TDP was that the locations of the deployed array sensors must be known with considerable accuracy, generally with an uncertainty of less than 1 m. This sensor localization requirement arose due to a need to accurately localize the source of signal energy, in particular, the depth of the source. This paper describes and demonstrates a technique referred to as Array Element Localization (AEL) that was developed to solve the sensor localization problem.

14. KEYWORDS, DESCRIPTORS or IDENTIFIERS (technically meaningful terms or short phrases that characterize a document and could be helpful in cataloguing the document. They should be selected so that no security classification is required. Identifiers, such as equipment model designation, trade name, military project code name, geographic location may also be included. If possible keywords should be selected from a published thesaurus. e.g. Thesaurus of Engineering and Scientific Terms (TEST) and that thesaurus-identified. If it not possible to select indexing terms which are Unclassified, the classification of each should be indicated as with the title).

AEL
Array Element Localization
Autonomous Processing
Inversion
Monte Carlo
Newton’s Method
Rapidly Deployable Systems
Ray Tracing
RDS
Regularized Solution
Underwater Acoustics

This page intentionally left blank.

Defence R&D Canada

Canada's leader in defence
and National Security
Science and Technology

R & D pour la défense Canada

Chef de file au Canada en matière
de science et de technologie pour
la défense et la sécurité nationale

www.drdc-rddc.gc.ca